

Oxygen defect accumulation at Si:HfO₂ interfaces

C. Tang and R. Ramprasad^{a)}

Department of Chemical, Materials and Biomolecular Engineering, Institute of Materials Science, University of Connecticut, 97 North Eagleville Road, Storrs, Connecticut 06269, USA

(Received 20 November 2007; accepted 8 April 2008; published online 9 May 2008)

It has been shown earlier that thermodynamic and kinetic driving forces exist for an isolated oxygen defect to segregate to Si:HfO₂ interfaces. In the present work, using the first principles calculations, we show that the accumulation of multiple point defects (O vacancies and interstitials) at Si:HfO₂ interfaces is also thermodynamically favored and this preference is relatively insensitive to the areal density of interfacial defects. These results indicate that the O point defect chemistry can provide a rationale for the formation of interfacial phases. © 2008 American Institute of Physics.

[DOI: 10.1063/1.2917576]

As prospective substitutes for conventional SiO₂ gate dielectrics, high dielectric constant (or high- κ) materials such as HfO₂ have been extensively studied. Due to its high thermodynamic stability in contact with Si,¹⁻³ HfO₂ is expected to be resistive to the formation of undesirable phases such as silica, silicates, and silicides at the Si:HfO₂ interface. However, in reality the formation of such interfacial phases have been observed.⁴⁻⁹ It has been proposed that these interfacial reactions could be closely related to high diffusivity of oxygen and due to deviations from the ideal stoichiometry of HfO₂ phases.¹⁰

Based on the first principles computations, we had shown earlier that isolated O vacancies¹¹ and interstitials¹² display strong thermodynamic and kinetic driving forces for segregation to the Si:HfO₂ interface. We found that an isolated O vacancy (interstitial) in bulk HfO₂ tends to relocate to the O (Si) layer closest to the Si:HfO₂ interface, potentially leading to the formation of interfacial Hf silicides (Si oxides).

While the above factors provide insights concerning the driving forces for the “nucleation” of new interfacial phases, larger scale accumulation of point defects at interfaces needs to be explicitly considered to address the formation of the uniform interfacial layers experimentally observed.^{5,9} In this work, based on density functional theory (DFT) computations, we estimate the thermodynamic driving force for the segregation of multiple O defects to the Si:HfO₂ interface from bulk HfO₂. The process modeled here is schematically shown in Fig. 1.

Our DFT calculations were performed using the VASP code¹³ with the Vanderbilt ultrasoft pseudopotentials,¹⁴ the generalized gradient approximation utilizing the PW91 functional,¹⁵ and a cutoff energy of 400 eV for the plane wave expansion of the wavefunctions. Bulk HfO₂ calculations involved a 2×2×2 supercell of monoclinic HfO₂ (*m*-HfO₂) containing 32 Hf and 64 O sites, and required a Monkhorst–Pack *k*-point mesh of 2×2×2 to yield converged results. All Si:HfO₂ computations involved a 2×2 interface unit cell, and hence, required a 2×2×1 Monkhorst–Pack mesh.

A wide range of interfacial area coverage by O defects

was considered. The formation energy *per O defect* can be formally defined as

$$E_f = (E_{\text{def}} - E_{\text{perf}} \pm n \times \mu_{\text{O}}) / n, \quad (1)$$

where E_{def} and E_{perf} represent the energies of the system with n O defects per supercell and the perfect system, respectively, and μ_{O} is the chemical potential of O. In Eq. (1), the plus and minus signs are for the vacancies and interstitials, respectively. The feasibility of the process shown in Fig. 1 for a given interfacial O defect density was estimated by determining ΔE_f , the difference between E_f at the Si:HfO₂ interface and the corresponding formation energy far away from the interface (i.e., in bulk HfO₂). Thus, ΔE_f does not explicitly depend on the actual choice of μ_{O} . For definiteness, we choose μ_{O} to be one-half energy of an isolated O₂ molecule when making explicit references to E_f . We do mention that the density of bulk defects at a given temperature will be controlled by the chemical potential of the ambient oxygen, as has been established before by the authors by using *ab initio* methods.¹⁶ In this work, we assume the prior existence of a certain density of bulk defects.

While the defects far away from the interface were treated by using bulk *m*-HfO₂ supercells (which were strained, see below), those at the interface were studied by using an explicit epitaxial interface model,^{11,12} in which the (001) surface of *m*-HfO₂ was stretched to coherently match that of Si [Fig. 2(a)]. The equilibrium *a*, *b*, and *c* lattice parameters of bulk *m*-HfO₂ were computed here to be 5.14, 5.19, and 5.30 Å, respectively, in good agreement with the corresponding experimental values of 5.12, 5.17, and 5.29 Å.¹⁷ The equilibrium lattice constant of crystalline Si was determined to be 5.46 Å, again in good agreement with

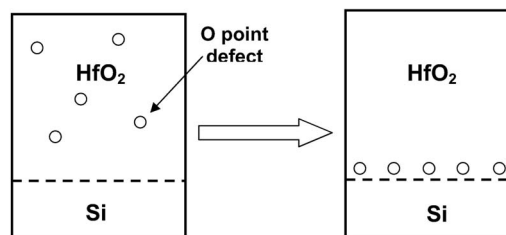


FIG. 1. Schematic illustration of the segregation of multiple O point defects from bulk HfO₂ to the Si:HfO₂ interface.

^{a)}Electronic mail: rampi@ims.uconn.edu.

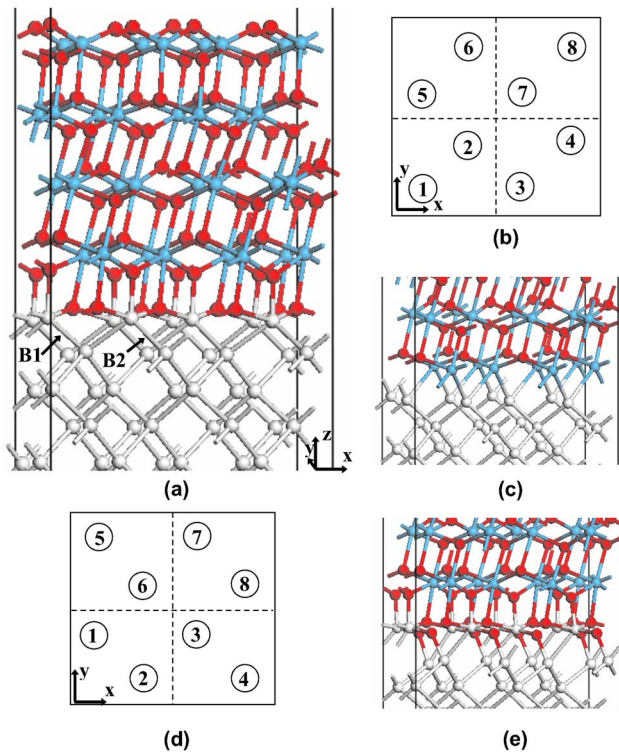


FIG. 2. (Color online) (a) Si:HfO₂ model with Si, Hf, and O atoms in white, blue (gray), and red (dark gray), respectively. (b) Interfacial O vacancy sites (top view). The dashed lines divide the interface into four equivalent cells. (c) Interfacial Hf silicide layer resulting due to an O vacancy AD of 2.0. (d) Interfacial O interstitial sites. Interstitials at sites 1 and 2 break bonds B1 and B2 shown in (a), respectively. (e) Interfacial SiO_x layer result due to an O interstitial AD of 1.0.

the experimental value of 5.43 Å.¹⁸ The epitaxial Si:HfO₂ model thus resulted in strains of 6% and 5% in the HfO₂ along the *a* and *b* directions.

First, we consider O defects far away from the interface, modeled here using bulk *m*-HfO₂ with *a* and *b* stretched to 5.46 Å (and with *c* optimized). Bulk *m*-HfO₂ contains threefold and fourfold coordinated O sites. We computed E_f for an isolated O vacancy [with $n=1$ in Eq. (1)] at the threefold and fourfold sites to be 6.41 and 6.20 eV, respectively, and that for an isolated O interstitial to be 0.95 and 0.66 eV, respectively. These calculations and those concerning isolated point defects in *equilibrium* HfO₂ are well documented elsewhere.^{12,16,19} Computations involving two O defects within a supercell indicate no significant change in E_f . For example, two O vacancies at fourfold sites separated by 5.46 and 2.89 Å display E_f of 6.23 and 6.20 eV per vacancy; likewise, two fourfold-site O interstitials separated by 5.46 and 3.78 Å display E_f of 0.67 and 0.83 eV per interstitial, respectively, within the E_f range of an isolated O interstitial.

Due to these factors, and as the deviation from perfect stoichiometry is generally small in bulk HfO₂,^{16,20} we use E_f of isolated O defects in bulk HfO₂ as a reference to quantify the thermodynamic driving force for the accumulation of O defects to the Si:HfO₂ interface.

Next, we consider the formation of multiple O defects at the Si:HfO₂ interface. The interface model [Fig. 2(a)] contained nine Si layers (eight atoms per layer) and four Hf layers. The dangling bonds of the top (Hf) and bottom (Si) free surfaces were passivated by adding half monolayer of O atoms²¹ and a vacuum of about 10 Å separated the whole structure from its image along the interface normal. We used the O-terminated interfaces as a starting point here, as these are more stable and desirable than the Hf-terminated ones in the absence of O defects.²¹ After geometry optimization, half of the interface O atoms contributed to the formation of the Si–O–Si bonds, while the other half resulted in the Hf–O–Hf bonds, thus, passivating all the interface dangling bonds.²¹ Oxygen defects were then created either by removing O atoms from the interfacial Si–O–Si bonds or by adding O atoms between the Si–Si bonds at the interface. These choices for the “final” locations of the defects were motivated by our prior work on isolated point defects which indicated these to be the minimum energy positions. In the present work, a range of interfacial defect areal densities (ADs) were considered. The areal ADs are defined here as the number of defects divided by 8, the number of interfacial O sites within the perfect Si:HfO₂ system [Fig. 2(a)]. An investigation of E_f with respect to the AD will indicate whether or not the defect accumulation process, which is critical to the interfacial phase formation, is energetically favorable. Note that E_f is defined per defect (both in bulk HfO₂ and at the Si:HfO₂ interface). This ensures that we always compare equivalent bulk and interface defect numbers.

Figure 2(b) schematically shows the interfacial O vacancy sites. Since the 2 × 2 interface can be divided into four equivalent 1 × 1 cells and each contains two inequivalent interfacial O sites, vacancy sites can be categorized into two groups: one indexed by odd numbers and the other by even numbers, as indicated in Fig. 2(b). We begin our discussion of E_f for interfacial O vacancies with a single vacancy per supercell at either sites 1 or 2 (AD=0.125). E_f was determined to be 5.29 and 5.12 eV for sites 1 and 2, respectively, about 1 eV lower than that in bulk HfO₂. Higher ADs were explored by considering 2, 4, 6, and 8 vacancies. Since it is challenging to exhaustively explore all possible combinations of vacancy locations for ADs between 0.125 and 1.0, only a few representative cases were chosen. The configurations were chosen to span the extreme cases of clustered and well-separated vacancies. The values of ΔE_f for all considered configurations and ADs are listed in Table I and plotted

TABLE I. Values of ΔE_f (eV per defect) with respect to O defect coverage at the Si:HfO₂ interface. Site label “1” is for a single defect at site 1, and site label “12” is for 2 defects at sites 1 and 2 simultaneously, and so on. E_f values for O vacancy (6.20 eV) and interstitial (0.66 eV) in the strained bulk HfO₂ were used as references to define ΔE_f .

1 vacancy	2 vacancies	4 vacancies	6 vacancies	8 vacancies	16 vacancies	1 interstitial	2 interstitials	4 interstitials	6 interstitials	8 interstitials	
Site	ΔE_f	Site	ΔE_f	Site	ΔE_f	Site	ΔE_f	Site	ΔE_f	Site	ΔE_f
1	-0.91	12	-1.18	2567	-1.14	135746	-1.20	-1.23	-1.41	1	-3.55
				2468	-1.11					12	-3.55
				4678	-1.18	246817	-1.21			1234	-3.54
										123456	-3.60
										1234567	-3.67
2	-1.08	13	-1.05							2	-3.50
										24	-3.44
										2468	-3.5
										123468	-3.58

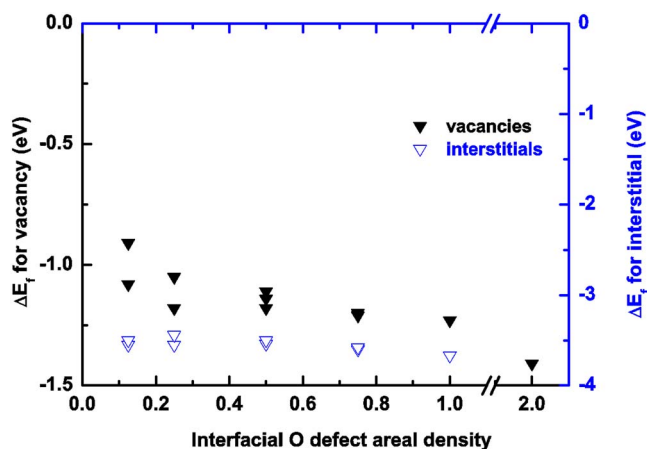


FIG. 3. (Color online) Relationship between ΔE_f and defect AD. Left axis is for vacancies and right axis is for interstitials.

in Fig. 3 (left axis). It can be seen that ΔE_f is always negative and that there is a slight but clear decrease in its value for increasing ADs. Thus, the approximately 1 eV driving force for segregation experienced by an isolated vacancy is maintained for multiple vacancies as well.

In addition, we considered a case that corresponds to a vacancy AD of 2.0, i.e., when the eight interfacial O atoms making up the Si–O–Si bonds as well as the eight O atoms in the layer above making up the Hf–O–Hf bonds are missing. Geometry optimization of this structure results in the formation of the Si–Hf bonds at the interface with bond lengths around 2.6 Å [Fig. 2(c)], close to the experimental Si–Hf bond length of 2.68 Å in bulk HfSi₂.²² Assuming that this interfacial “silicide” layer is formed due to the accumulation of O vacancies, we obtain an E_f of about 1.4 eV below that in bulk HfO₂ and about 0.2 eV below that in the case of AD=1.0. Thus, it is evident that although the O-terminated Si:HfO₂ interface is stable in the absence of O defects, multiple O vacancies from bulk HfO₂ (when present) tend to segregate to the Si:HfO₂ interface and could result in interfacial Hf silicides.

Next, we consider the accumulation of O interstitials at the Si:HfO₂ interface. The labeling method similar to that adopted for vacancies was used to index the interfacial interstitial sites [Fig. 2(d)]. For instance, interstitial sites 1 and 2 are in between the interfacial Si–Si bonds [indicated as B1 and B2 in Fig. 1(a)] and form the Si–O–Si bonds. Again, we start our E_f calculations with the case of an isolated O interstitial corresponding to AD=0.125. In this case, E_f are –2.89 and –2.84 eV for sites 1 and 2 respectively, which are lower than the corresponding bulk values by more than 3.5 eV. By employing the same strategy for the vacancy cases discussed

above, we explored higher ADs (0.25, 0.5, 0.75, and 1.0) by adding two, four, six, and eight O atoms at the interface. For these representative cases, the large driving force for segregation (i.e., large negative ΔE_f value) experienced by an isolated O interstitial is well maintained, as listed in Table I and illustrated in Fig. 3 (right axis). From a thermodynamic point of view, we conclude that multiple O interstitials tend to segregate from bulk HfO₂ to the Si:HfO₂ interface, which could result in an interfacial SiO_x layer. As an example, the SiO_x layer corresponding to AD=1.0 is shown in Fig. 2(e).

In summary, we have studied the relation between the thermodynamic driving force for O defect migration to the Si:HfO₂ interface and the defect ADs at the interface. Our results clearly indicate that when multiple O defects are present in the HfO₂ film (as specified by the ambient oxygen pressure or chemical potential), they tend to accumulate at the interface and form interfacial phases.

The authors would like to acknowledge the financial support of this work by the ACS Petroleum Research Fund and the National Science Foundation.

¹R. M. Wallace and G. D. Wilk, *Crit. Rev. Solid State Mater. Sci.* **28**, 231 (2003).

²J. Robertson, *Rep. Prog. Phys.* **69**, 327 (2006).

³J.-P. Locquet, C. Marchiori, M. Sousa, J. Fompeyrine, and J. W. Seo, *J. Appl. Phys.* **100**, 051610 (2006).

⁴D. Y. Cho, K. S. Park, B. H. Choi, S. J. Oh, Y. J. Chang, D. H. Kim, T. W. Noh, R. Jung, J. C. Lee, and S. D. Bu, *Appl. Phys. Lett.* **86**, 041913 (2005).

⁵H. S. Baik, M. Kim, G.-S. Park, S. A. Song, M. Varela, A. Franceschetti, S. T. Pantelides, and S. J. Pennycook, *Appl. Phys. Lett.* **85**, 672 (2004).

⁶R. Jiang, E. Q. Xie, and Z. F. Wang, *Appl. Phys. Lett.* **89**, 142907 (2006).

⁷J. C. Lee, S. J. Oh, M. J. Cho, C. S. Hwang, and R. J. Jung, *Appl. Phys. Lett.* **84**, 1305 (2004).

⁸X. Y. Qiu, H. W. Liu, F. Fang, M. J. Ha, and J. M. Liu, *Appl. Phys. Lett.* **88**, 072906 (2006).

⁹N. Miyata, *Appl. Phys. Lett.* **89**, 102903 (2006).

¹⁰S. Stemmer, *J. Vac. Sci. Technol. B* **22**, 791 (2004).

¹¹C. Tang, B. Tuttle, and R. Ramprasad, *Phys. Rev. B* **76**, 073306 (2007).

¹²C. Tang and R. Ramprasad, *Phys. Rev. B* **75**, 241302(R) (2007).

¹³G. Kresse and J. Furthmüller, *Phys. Rev. B* **54**, 11169 (1996).

¹⁴D. Vanderbilt, *Phys. Rev. B* **41**, R7892 (1990).

¹⁵J. P. Perdew, J. A. Chevary, S. H. Vosko, K. A. Jackson, M. R. Perderson, D. J. Singh, and C. Fiolhais, *Phys. Rev. B* **46**, 6671 (1992).

¹⁶C. Tang and R. Ramprasad, *Appl. Phys. Lett.* **91**, 022904 (2007).

¹⁷J. Adam and M. D. Rodgers, *Acta Crystallogr.* **12**, 951 (1959).

¹⁸C. R. Hubbard, H. E. Swanson, and F. A. Mauer, *J. Appl. Crystallogr.* **8**, 45 (1975).

¹⁹A. S. Foster, F. Lopez Gejo, A. L. Shluger, and R. M. Nieminen, *Phys. Rev. B* **65**, 174117 (2002).

²⁰N. M. Tallan, W. C. Tripp, and R. W. Vest, *J. Am. Ceram. Soc.* **50**, 279 (1967).

²¹P. W. Peacock, K. Xiong, K. Tse, and J. Robertson, *Phys. Rev. B* **73**, 075328 (2006).

²²J. F. Smith and D. M. Bailey, *Acta Crystallogr.* **10**, 341 (1957).